Contents

This page intentionally left blank

All models are wrong but some are useful.

Robustness in the Strategy of Scientific Model Building
George Box, 1979

Chapter 5

Online assessment of the parametrised model

In Chapter 4, I analysed the subgrid tendencies and constructed a statistical model (4.6) to estimate them from the coarse model tendencies. In this chapter, I will assess the performance of the parametrised model obtained by coupling the statistical model into the coarse Rayleigh-Bénard model.

First, a "truth" solution was obtained by running the fine (i.e., 2048×256; see Table 4.1) model for 300 time units, saving the output at intervals of 0.2 time units. The last snapshot from the fine model simulation described in § 4.1 (Step 1) was used as the initial condition, thus keeping the data used to test the parametrisation separate from the data used to fit it. Every snapshot in the truth dataset was then coarse-grained using the method described in § 4.2; the aim is for the parametrised model to approximate this coarse-grained truth solution as closely as possible.

A control solution was obtained by running the unmodified coarse (i.e., 256×64) model, using the first coarse-grained snapshot of the truth solution as an initial condition. Output was saved at approximately the same interval of 0.2 time units.

The equations governing the parametrised model, given schematically by (4.5), can be written out explicitly as

$$\begin{aligned}
\frac{\partial \boldsymbol{u}}{\partial t} &= \begin{pmatrix} 1 + f_u(z) & 0 \\ 0 & 1 + f_w(z) \end{pmatrix} \left[-\boldsymbol{u} \cdot \boldsymbol{\nabla} \boldsymbol{u} - \boldsymbol{\nabla} \pi + \left(\frac{\mathrm{Pr}}{\mathrm{Ra}} \right)^{1/2} \left(\nabla^2 \boldsymbol{u} + \tilde{\nu} f(z) |\nabla^2 \boldsymbol{u}| \nabla^2 \boldsymbol{u} \right) + \theta \hat{\boldsymbol{z}} \right], \\
\frac{\partial \theta}{\partial t} &= (1 + f_\theta(z)) \left[-\boldsymbol{u} \cdot \boldsymbol{\nabla} \theta + (\mathrm{Ra}\,\mathrm{Pr})^{-1/2} \left(\nabla^2 \theta + \tilde{\kappa} f(z) |\nabla^2 \theta| \nabla^2 \theta \right) \right], \quad \text{and} \\
\boldsymbol{\nabla} \cdot \boldsymbol{u} &= 0,
\end{aligned}$$

where the terms in red distinguish these modified equations from the originals (3.13)–(3.15). The parametrised model was run with the same resolution, time step, initial condition and output interval as the control.

Unfortunately, when the parametrised model was run with the f_θ, f_u and f_w that were fitted in § 4.4, it became unstable and crashed within 10 time units. Given the low coefficients of determination for the u and w fits (Table 4.2), I chose to set $f_u(z) = f_w(z) \equiv 0$—that is, to only parametrise the θ tendency and leave the momentum equation unmodified. This stabilised the model.

5.1 Short-term forecast accuracy

I first assess short-term accuracy using the root-mean-square error (RMSE) of u, w and θ, defined by

$$\mathrm{RMSE}_\chi(t) = \sqrt{\langle[\chi_{\mathrm{fc}}(t) - \chi_{\mathrm{truth}}(t)]^2\rangle_{x,z}},$$

where $\chi = u, w, \theta$, χ_{fc} is the forecast generated by either the control or parametrised model and χ_{truth} is the *coarse-grained* truth solution. Figure 5.1 (a-c) compares the RMSE of the control and parametrised solutions for the first 70 time units of simulation.

Panel (a) shows that the θ RMSE of the parametrised model initially grows at less than half the rate seen in the control, remaining smaller than the control value for almost 10 time units before surpassing it. While both models reach a peak RMSE before settling to a steady equilibrium, the parametrised model takes approximately four times longer to do so. It seems likely that by reducing the magnitude of $\partial\theta/\partial t$ near the top and bottom of the domain, the parametrisation preserves the properties of the thermal boundary layers. These are relatively thick and slowly-evolving in the coarse-grained truth solution, but are thinned too quickly by the control model.

For u and w, the RMSE of the parametrised model initially increases at a rate much closer to that of the control model. However, by plotting the difference between the two and zooming the time axis (panels d-f), it can be seen that the parametrised model does indeed have a slightly smaller error.

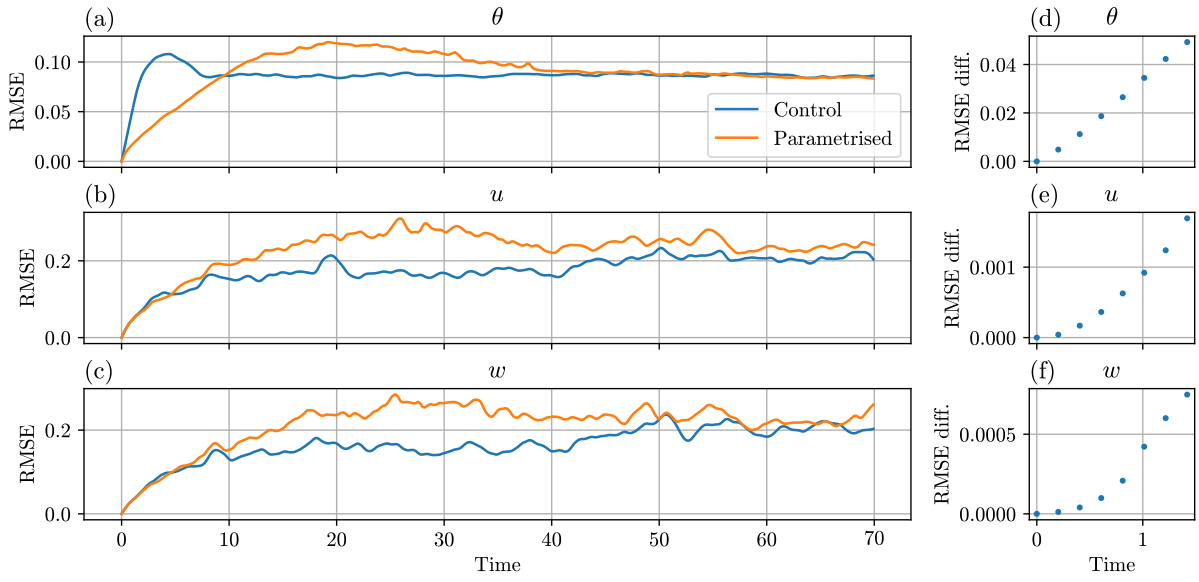

Figure 5.1: **(a-c):** Root-mean-square error of the control (blue) and parametrised (orange) solutions for θ, u and w over the first 70 time units of simulation. **(d-f):** The control RMSE minus the parametrised RMSE over the first 1.5 time units, confirming that the parametrised solution has lower RMSE in the short term.

Another way to assess short-term accuracy is to calculate domain-averaged quantities for the parametrised, control and truth solutions and compare them over time. As in § 3.6, I consider the Nusselt number Nu, thermal boundary layer thickness δ_θ, RMS speed u_{rms}, kinetic energy dissipation rate ϵ_k and thermal dissipation rate ϵ_θ, plotting their time series in Figure 5.2. Both the control and parametrised models make grossly inaccurate predictions for δ_θ and ϵ_θ, but the parametrised model's predictions are nonetheless closer to the truth for the first $\sim$ 20 time units. Since these are purely thermal quantities, their improved prediction can be attributed to the nature of the parametrisation scheme in the same way as the θ RMSE. The parametrised model also makes more accurate initial predictions for the other three quantities, but only for the first $\sim$ 5 time units.

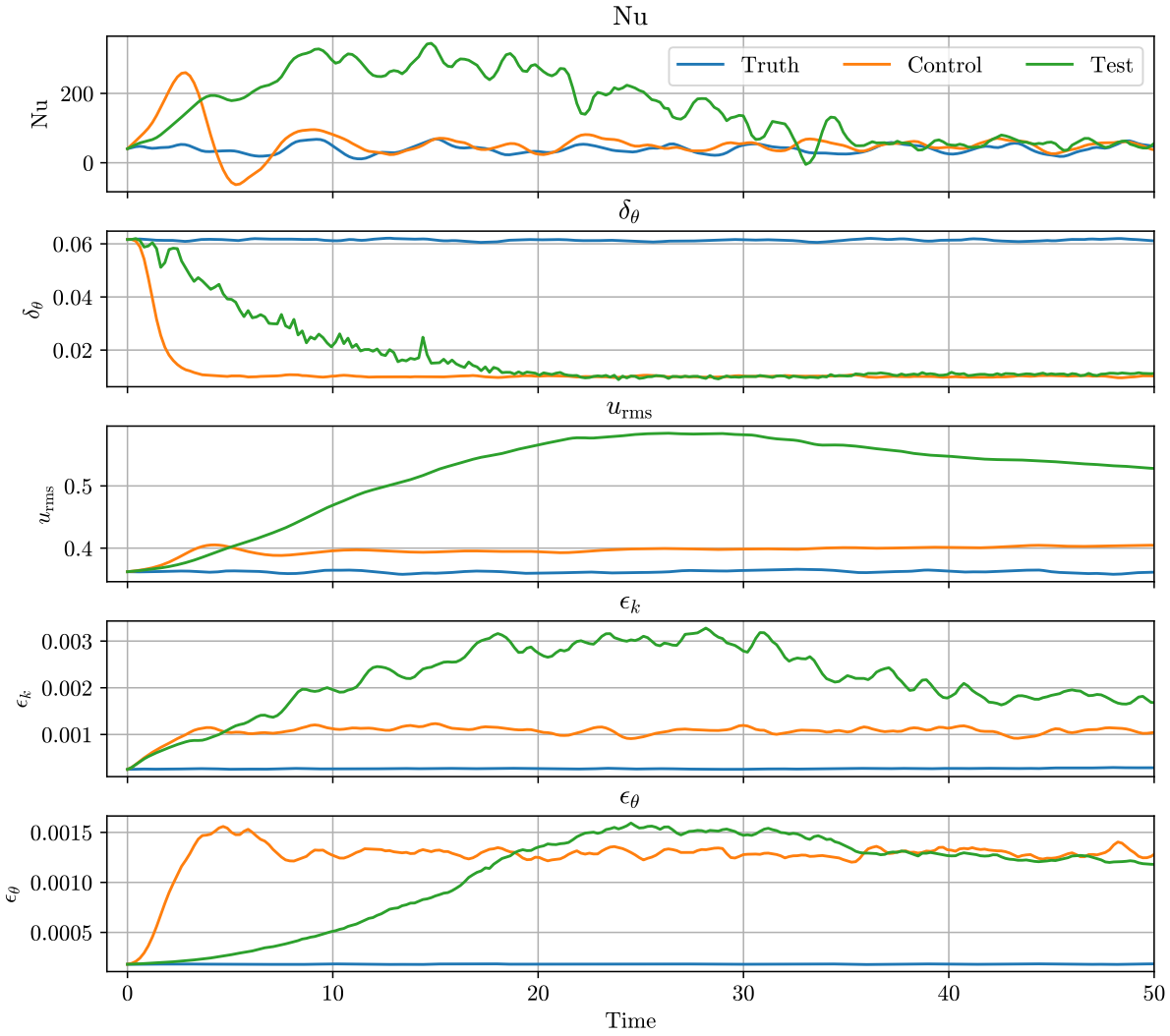

Figure 5.2: Time series of the Nusselt number Nu, thermal boundary layer thickness δ_θ, RMS speed u_{rms}, kinetic energy dissipation rate ϵ_k and thermal dissipation rate ϵ_θ for the coarse-grained truth (blue), control (orange) and parametrised (green) solutions over the first 50 time units.

So far, I have shown that the parametrised model is capable of producing more accurate short-term forecasts than the control if the lead time is sufficiently short (on the order of a few time units)—a promising result.

5.2 Long-term statistical accuracy

I next consider the long-term mean properties of the parametrised model once it is allowed to reach a statistically steady state. This required 1100 time units of simulation, with the first 800 time units of data being discarded (see Appendix B.2.1). For consistency, the control solution was also extended to 1100 time units. The fine model did not require further spin-up, having been initialised in a statistically steady state.

It is insightful to first compare the steady-state solutions qualitatively. Figure 5.3 shows that the coarse-grained temperature field of the fine truth solution (panel (a)) is smooth and well-resolved. In particular,

it has a thermal boundary layer thickness on the order of 0.1. The control model, despite being initialised from a coarse-grained state like the one in Figure 5.3a, reverts to a state where the temperature field is poorly resolved and the thermal boundary layers are much thinner. Notably, the parametrised solution is much closer in appearance to the control than the coarse-grained truth, which it is supposed to represent.

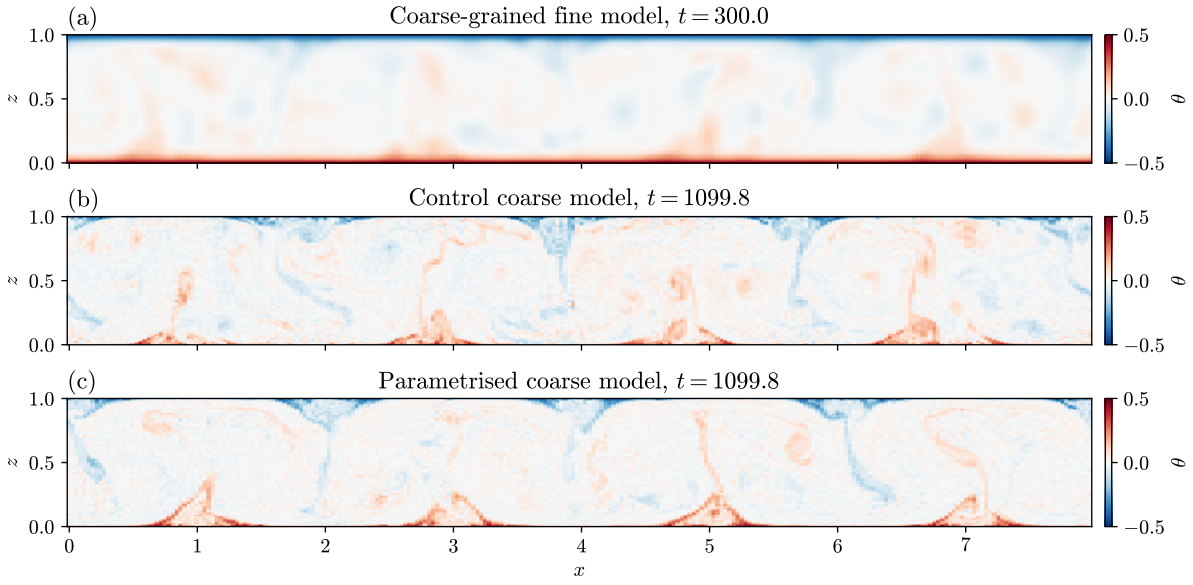

Figure 5.3: Example temperature snapshots in the statistically steady regime for **(a)** the coarse-grained truth solution (which the parametrised solution should ideally resemble), **(b)** the control solution and **(c)** the parametrised solution.

The core issue is the smoothing involved in the coarse-graining operation. On the one hand, I explained in § 4.2 that insufficient smoothing causes artefacts that mask the subgrid tendency signal, making it more difficult to model the subgrid tendencies. On the other hand, Figure 5.3 shows that the natural state of the coarse model is not smooth. By parametrising the θ subgrid tendency, I have attempted to force the coarse model towards the coarse-grained truth solution, and although this is successful for a short time (as shown in § 5.1), the parametrised model eventually settles to a state that is grossly unrepresentative of the target. It is clear that future work will need to consider more sophisticated parametrisation schemes in order to resolve this problem. Such a scheme might contain a diffusion term to further smooth the coarse solution.

Despite the above issues, I proceed to perform a similar analysis to § 3.6, calculating the time averages of Nu, δ_θ, u_{rms}, ϵ_k and ϵ_θ over 300 time units for the coarse-grained truth, control and parametrised solutions. I stress that the high-resolution truth solution was first coarse-grained before the metrics were calculated. Uncertainties were estimated using the same method of running means (3.21) and rolling means (3.22) with a 150-time-unit window.

Figure 5.4 shows that parametrisation has resulted in a statistically significant improvement across all five metrics, approximately halving the relative error for Nu and u_{rms}. Both the control and parametrised solutions have very large errors for δ_θ ($\sim -80\%$), ϵ_k ($\sim 300\%$) and ϵ_θ ($\sim 500\%$)—an unsurprising result, given the issue discussed earlier in this section—but the relative errors of the parametrised solution are nonetheless smaller than those of the control.

Given that the parametrised solution is generally unrepresentative of the coarse-grained truth, one may alternatively ask how close its long-term statistics are to those of the *uncoarsened* high-resolution truth data. I repeat the previous analysis, now calculating the truth solution metrics without first coarse-graining the data. Figure 5.5 shows that parametrisation produces a statistically significant reduction in the magnitude of the relative error for Nu, δ_θ and u_{rms}. There is no significant change in magnitude (but

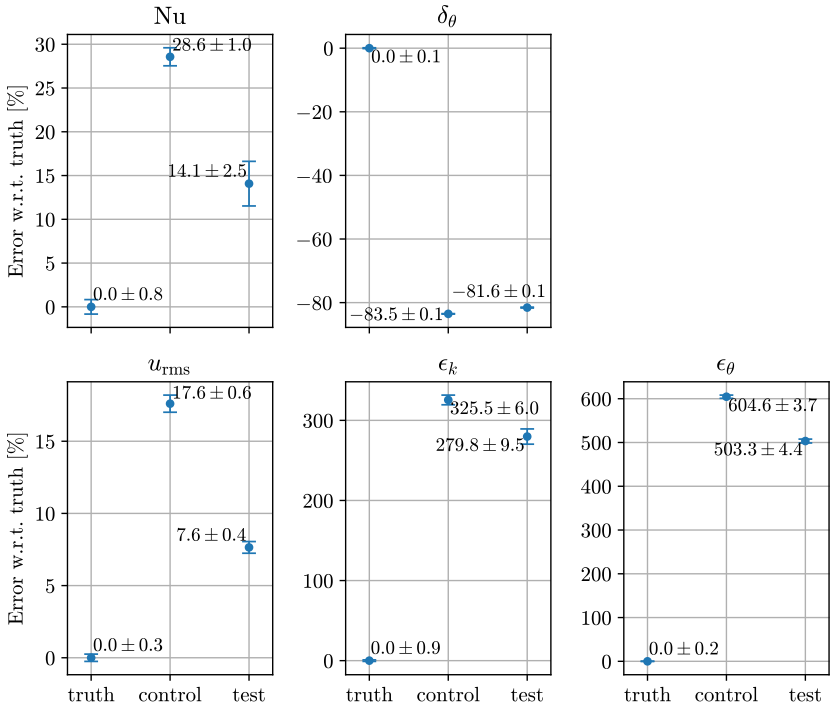

Figure 5.4: Time-averaged Nusselt number Nu, thermal boundary layer thickness δ_θ, RMS speed u_{rms}, kinetic energy dissipation rate ϵ_k and thermal dissipation rate ϵ_θ for the coarse-grained truth, control and parametrised ("test") solutions. Values are expressed as percentage errors relative to truth.

a change of sign) for ϵ_k and an increase in magnitude with change in sign for ϵ_θ. This is a surprising result because the parametrisation scheme is not explicitly designed to improve the coarse model in comparison to the uncoarsened fine model (only the coarse-grained fine model). In fact, this type of improvement is arguably more useful for practical applications; to give an analogy, a coarse-resolution climate model that directly reproduces the spatially-averaged statistics (surface temperature, precipitation rate, etc.) of a finer model could be more useful than one that reproduces those of the coarsened and smoothed fine model output.

As a final note, the integration of the fine model required approximately 120 CPU-hours of wall time per 100 units of model time, while the control and parametrised models required approximately 1.6 CPU-hours and 1.7 CPU-hours per 100 units of model time respectively. This indicates that the parametrised model's improved predictive skill comes at little to no additional overhead cost compared to the control.

TODO: summary?

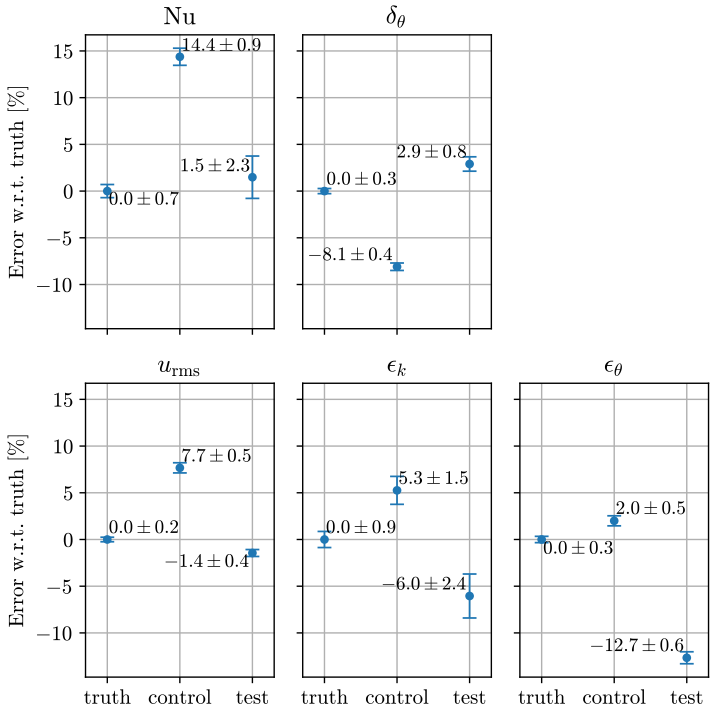

Figure 5.5: As for Figure 5.4, except that the truth values are computed *without* first coarse-graining the high-resolution data.